9-1-2010

Kinetics of DNA and RNA Hybridization in Serum and Serum-SDS

Elton Graugnard
Boise State University

Amber Cox
Boise State University

Jeunghoon Lee
Boise State University

Cheryl Jorcyk
Boise State University

Bernard Yurke
Boise State University

See next page for additional authors

 DOI: 10.1109/TNANO.2010.2053380

Kinetics of DNA and RNA Hybridization in Serum and Serum-SDS

Elton Graugnard, Amber Cox, Jeunghoon Lee, Cheryl Jorcyk, Bernard Yurke, and William L. Hughes

***Abstract*—Cancer is recognized as a serious health challenge both in the United States and throughout the world. While early detection and diagnosis of cancer leads to decreased mortality rates, current screening methods require significant time and costly equipment. Recently, increased levels of certain micro-ribonucleic acids (miRNAs) in the blood have been linked to the presence of cancer. While blood-based biomarkers have been used for years in cancer detection, studies analyzing trace amounts of miRNAs in blood and serum samples are just the beginning. Recent developments in deoxyribonucleic acid (DNA) nanotechnology and DNA computing have shown that it is possible to construct nucleic-acid-based chemical networks that accept miRNAs as inputs, perform Boolean logic functions on those inputs, and generate as an output a large number of DNA strands that can be readily detected. Since miRNAs occur in blood in low abundance, these networks would allow for amplification without using polymerase chain reaction. In this study, we report initial progress in the development of a DNA-based cross-catalytic network engineered to amplify specific cancer-related miRNAs. Subcomponents of the DNA network were tested individually, and their operation in serum, as well as a mixture of serum with sodium dodecyl sulfate, is demonstrated. Preliminary simulations of the full cross-catalytic network indicate successful operation.**

***Index Terms*—Cancer, catalytic, chemical cascade, chemical network, detection, diagnosis, deoxyribonucleic acid (DNA), entropy driven, microribonucleic acid (miRNA), strand invasion.**

I. Introduction

WORLDWIDE, there are approximately 1.3 million lung cancer deaths per year [1]. The lives of many individuals could be improved and/or saved by earlier detection and accessibility to simple detection methods, particularly in remote locations. Early detection of cancer and decreased mortality rates are improved by screening technologies [2]. Lung cancer research seeks a noninvasive screening test capable of improving survival outcomes via early stage detection.

Microribonucleic acids (miRNAs) are small, single-stranded, noncoding RNAs that are 21–23 nucleotides in length. As gene regulators, they either suppress the translation or accelerate the degradation of target messenger RNAs (mRNAs) by binding to the 3′ untranslated regions [3], [4]. It is estimated that some miRNAs control hundreds of gene targets, and miRNAs are involved in the regulation of ∼30% of all genes and nearly every genetic pathway [5]. Evidence also suggests that miRNAs can function as oncogenes or tumor suppressors [6]–[8]. Besides their roles in tumor initiation, miRNAs have been found to play critical roles in several aspects of tumor progression and metastasis. Furthermore, several miRNAs and the components of miRNA pathways are amplified in some cancers [9]. Hence, miRNAs and the components of the miRNA pathway can serve as targets for early cancer detection, as well as for the discovery of anticancer agents.

Recently, it has been shown that miRNAs can be detected in human blood serum [10]. miRNA expression profiling reveals that miRNA signatures can be used for cancer classification and prognosis [11]–[13]. For example, miR-25 and miR-223 are highly expressed in the serum of lung cancer patients [10]. Current diagnosis technology requires the isolation of total RNA, production of complementary deoxyribonucleic acid (cDNA), and quantitative polymerase chain reaction (PCR) to detect these miRNAs in serum. However, recent studies have shown that metastable DNA systems exhibiting catalytic behavior, either autocatalytic or cross catalytic, can be constructed, thus giving rise to exponential amplification with large demonstrated amplification [14], [15]. Since miRNAs occur in serum in low abundance, these systems would allow for amplification without using PCR. Here, we present the initial design of a metastable cross-catalytic DNA system that rearranges to a stable configuration upon the input of a specific catalyst miRNA and produces, as an output signal, strands that generate easily detectable fluorescence.

By adopting the methodology and labeling convention created by Zhang *et al*. [15], the cross-catalytic DNA system shown in Fig. 1 was designed to detect and amplify a specific miRNA. The cross-catalytic system is composed of four distinct components: the "translator" [see Fig. 1(a)], the "cross-catalytic network" [see Fig. 1(b)] and two "reporter" complexes [see Fig. 1(c) and (d)], each consisting of various DNA strands with specific domains. The domains correspond to specific DNA sequences and are designated by letters or numbers. Subdomains are indicated with an appended letter (i.e., domain "**9**" consists

Manuscript received December 8, 2009; revised May 25, 2010; accepted June 7, 2010. Date of publication June 21, 2010; date of current version September 9, 2010. This work was supported by the National Institutes of Health under Grant P20 RR016454 and by the National Science Foundation under Computing and Communication Foundations Grant 0855212. The review of this paper was arranged by Associate Editor J. Li.

E. Graugnard, A. Cox, and W. L. Hughes are with the Department of Materials Science and Engineering, Boise State University, Boise, ID 83725 USA (e-mail: willhughes@boisestate.edu).

J. Lee is with the Department of Chemistry and Biochemistry, Boise State University, Boise, ID 83725 USA.

C. Jorcyk is with the Department of Biological Sciences, Boise State University, Boise, ID 83725 USA.

B. Yurke is with the Departments of Materials Science and Engineering and Electrical and Computer Engineering, Boise State University, Boise, ID 83725 USA.

Color versions of one or more of the figures in this paper are available online at http://ieeexplore.ieee.org.

Digital Object Identifier 10.1109/TNANO.2010.2053380

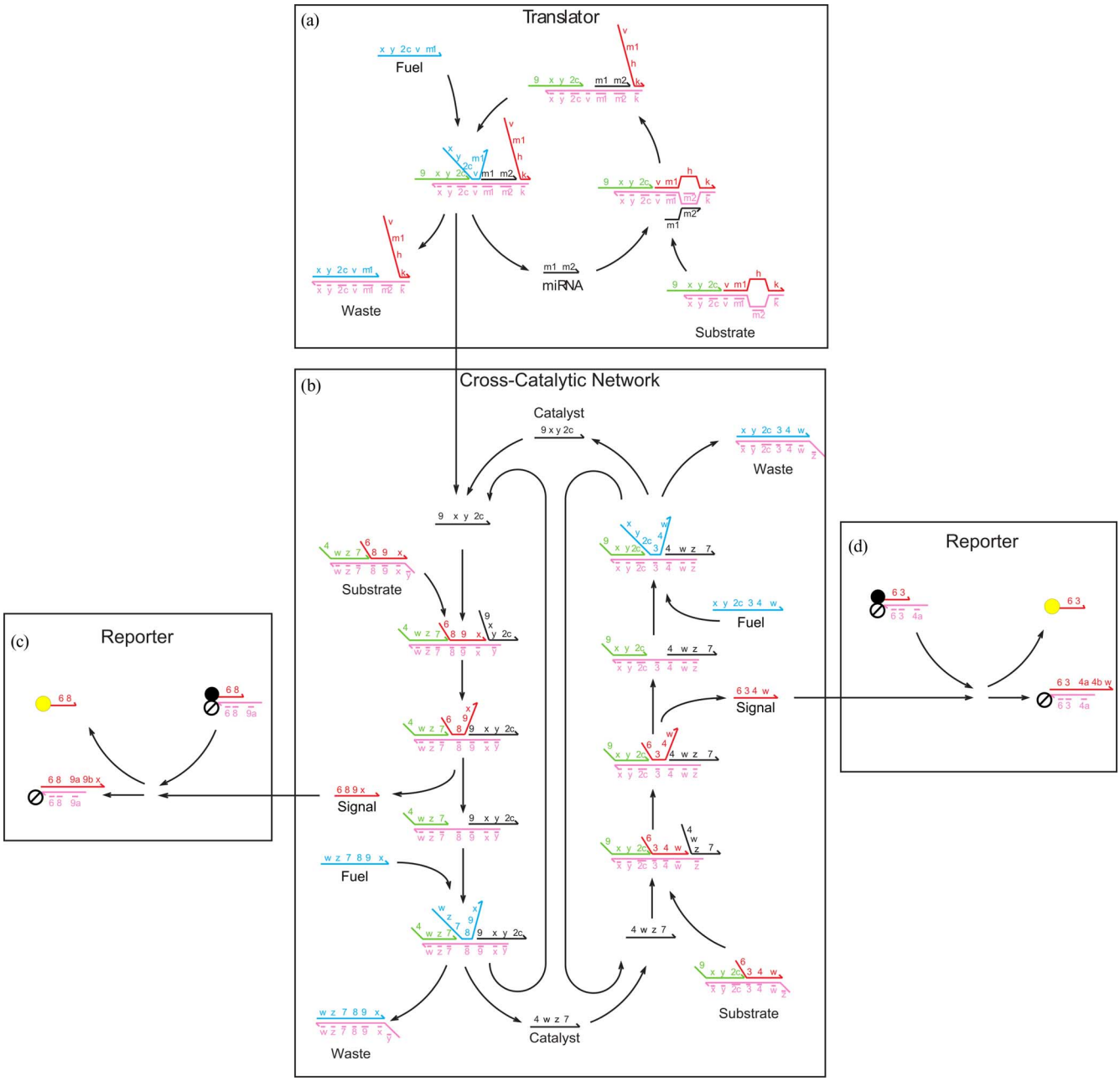

Fig. 1. Cross-catalytic DNA system for amplifying a specific miRNA. (a) Translator network is an autocatalytic system, whose output strand increases linearly with time. (b) Output of the translator network serves as one of the two catalysts in the cross-catalytic network, which releases signal strands whose concentration increases exponentially with time. (c) and (d) Signal strands invade dye-quencher reporter complexes to yield a rapid, easily detectable fluorescent signal. The yellow circle represents a dye molecule, the circle with a bar represents a quencher molecule, and the black circle represents a quenched dye.

of "**9a**" and "**9b**"). Complementary domains are shown with a bar over the domain name (i.e., domain "$\bar{\mathbf{9}}$" is the complement to "**9**"). The strands have also been color coded according to their function: catalytic input (black), catalytic output (green), substrate (pink), fuel (blue), and signal (red).

The translator network [see Fig. 1(a)] consists of several DNA complexes that include: 1) a "miRNA" catalyst strand; 2) a "substrate" complex of three strands; 3) a "fuel" strand; and 4) a "waste" complex. The miRNA catalyst is divided into two domains **m1** and **m2** and triggers a chemical cascade, via strand invasion, without being consumed or altered by the substrate complex [15]. During chemical amplification, the substrate complex is converted into a waste product through interaction with a DNA fuel strand. In the absence of a catalyst, this interaction is inhibited because the complement of the fuel is protected by the **9 x y 2c** strand and a portion of the **v m1 h k** strand. By interacting with an internal "toehold," the catalyst is able to expose a domain with which the "**v**" domain of the fuel strand can hybridize to its complement in an intermediate configuration. Strand displacement by the fuel then produces a waste product and releases the **9 x y 2c** output strand and the original miRNA catalyst.

The **9 x y 2c** strand from the translator acts as a catalyst in the cross-catalytic network [see Fig. 1(b)]. Operation of the two catalytic loops of the cross-catalytic network is equivalent, so it suffices to describe the function of one in detail. Consider the left-hand catalytic loop of the network. The DNA strand **9 x y 2c** functions as a catalyst that in the presence of a fuel strand **w z 7 8 9 x** operates on the substrate complex consisting of the strands **4 w z 7** and **6 8 9 x** hybridized to strand $\overline{\mathbf{w}}\ \overline{\mathbf{z}}\ \overline{\mathbf{7}}\ \overline{\mathbf{8}}\ \overline{\mathbf{9}}\ \overline{\mathbf{x}}\ \overline{\mathbf{y}}$, given in this case from the 3′ to 5′ direction. The overall reaction results in the release of the signal strand **6 8 9 x** and the strand **4 w z 7**, which functions as the catalyst for the right-hand catalytic loop of the network. Four intermediates of the left-hand loop are displayed in Fig. 1(b). Following the sequence of reactions from top to bottom in Fig. 1, the first intermediate is formed when the catalyst strand **9 x y 2c** attaches itself, via the "**y**" domain, to the complementary overhang on the substrate. The second intermediate results when the attached catalyst strand competes with the signal strand **6 8 9 x** for binding with the pink strand of the substrate complex. This process involves reversibly passing through a number of transitions via three-way branch migration. During branch migration, domains **9 x y** of the catalyst strand hybridize with the pink substrate and the signal strand is attached to the substrate complex only via domain "**8**," which is short, consisting of only four nucleotides. With high probability this substrate complex dissociates, releasing the signal strand **6 8 9 x** and forming the third intermediate, containing an exposed "$\overline{\mathbf{8}}$" domain. The exposed domain provides an attachment site onto which the fuel strand **w z 7 8 9 x** hybridizes via the "**8**" domain, shown as the fourth intermediate in Fig. 1(b). As a consequence of three-way branch migration, the fuel strand displaces the catalyst and the output strands. Once displaced, the output strand functions as a catalyst for the right-hand catalytic loop. During each half-cycle of the cross-catalytic network, a fuel strand is consumed, a waste complex is created, and three strands are released: the original half-cycle catalyst strand, an output strand that catalyzes the next half-cycle, and a signal strand. By proper design of the strand domains, the uncatalyzed system will remain indefinitely in the metastable state.

Note that the catalyst strand is not consumed in the overall reaction, i.e., it functions as its name implies. The catalyst serves to initiate the overall reaction, whereby the substrate complex and the fuel strand are converted into a signal strand, an output strand, and a waste product. All the intermediate reactions involved in this transformation are reversible. The net change in the number of base pairs in the overall reaction is zero. Thus, the reaction is not driven forward enthalpically, but rather by a net gain in entropy, as the system goes from two components (the fuel strand and the substrate complex) to three components (the signal strand, the output strand, and the waste product). This entropic gain has been shown to be sufficient to drive the system forward against a decrease of eight base pairs [15].

Since the output strand of each catalytic half-cycle of Fig. 1(b) serves as a catalyst strand for the other half-cycle, the production of new catalyst is proportional to the catalyst concentration. This process gives rise to exponential growth of the catalyst concentration, until depletion of the fuel or substrate strands becomes significant. Since the number of signal strands produced is proportional to the substrates consumed, they also exhibit exponential growth. Fig. 1(c) and (d) shows the reporter complexes, which release dye-labeled DNA strands upon strand invasion of the dye-quencher pairs by signal strands **6 8 9 x** and **6 3 4 w**. Thus, the exponential increase in signal strands will result in a rapid, easily detectable fluorescent signal.

II. Experimental Methods

Considerable literature exists on the degradation of nucleic acids by nucleases in body fluids and on methods by which nucleic acids can be made resistant to nuclease activity, especially for blood [16]–[25]. However, additional studies are required to address stability and rate issues relevant to the design of catalytic DNA networks for operation in serum or other body fluids. Rate constants for hybridization reactions are of particular interest, as are rates of degradation of nucleic acids due to nuclease activity. Initial experiments were performed to compare hybridization rates of nucleic acids in phosphate-buffered saline (PBS) solution and human blood serum. The use of sodium dodecyl sulfate (SDS) added to serum was explored as a means to suppress nuclease activity without disrupting DNA hybridization. Additionally, operation of the cross-catalytic network has been confirmed through simulation.

Initial experiments were performed to determine hybridization rates using the following set of three single-stranded DNA sequences:

F (fluorescent):
5′-(TET)-AAACCGTTACCATTACTGAGTT-3′Q
(quencher):
5′-GTAGTGTGGGAACTCAGTAATGGTAACGGTTT-(Iowa Black FQ)-3′
I (invader):
5′-AAACCGTTACCATTACTGAGTTCCCACACTAC-3′

Each custom strand was purchased and purified from Integrated DNA Technologies, Inc. Stock solutions were prepared by resuspending the strands in pure water at a nominal concentration of 100 μM. The fluorescent strand F, shown red in Fig. 2, consisted of a 22-nucleotide-long sequence labeled with tetrachlorofluorescein (TET) dye at the 5′ end (yellow circle). The emission maximum of the TET dye occurs near 538 nm. The quencher strand Q, shown blue in Fig. 2, consisted of a 32-nucleotide-long sequence labeled with Iowa Black fluorescence quencher at the 3′ end (circle with bar). The absorption maximum of the quencher occurs near 531 nm. The invader strand I was an unlabeled 32-nucleotide sequence and was fully complementary to the quencher strand Q.

All experiments were performed at 20 °C with DNA concentrations ranging from 2.5 to 50 nM, as determined by absorption measurements. Control experiments were performed in 1× PBS, consisting of 0.01 M phosphate buffer and 0.154 M sodium chloride with a pH of 7.4, purchased from Sigma-Aldrich, Inc. Experiments testing hybridization in serum were performed in three separate solutions: 1) 50% serum, consisting of 1× PBS and human serum mixed in equal volumes; 2) 10% SDS, consisting of 1× PBS mixed with 10 wt% SDS; and 3) 50% serum/10% SDS, consisting of a solution of 1× PBS

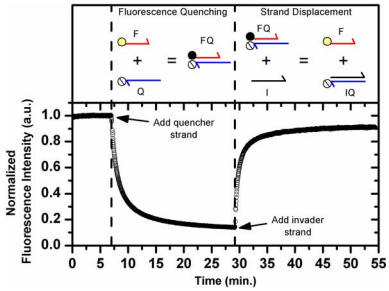

Fig. 2. Hybridization and strand displacement kinetics using FRET. The data are for the fluorescent (F), quencher (Q), and invader (I) strands at 20 °C in 1× PBS buffer. The base sequences for the strands are given in the text. The initial sample contained strand F. Strand Q was added to the solution at ∼7 min and hybridized with F, as indicated by the decrease in fluorescent intensity resulting from FRET. At ∼29 min, strand I was added to the solution. The presence of an available toehold on strand Q allowed the longer I strand to invade the hybridized dye-quencher pair FQ, robbing the quencher from the dye and allowing the fluorescence intensity to increase. Strand concentrations were nominally 50 nM.

with 20 wt% SDS mixed with an equal volume of human serum. Fluorescence intensity versus time was measured using a Varian Cary Eclipse spectrofluorometer with standard, plastic 10-mm cuvettes.

To prepare human serum, whole blood was collected in glass vacutainer tubes. The blood was allowed to clot in the collection tubes at room temperature for 30 to 60 min. The tubes were centrifuged at 1100–3000 rev/min for 10 min at room temperature. One milliliter aliquots of clear serum were transferred to separate tubes and stored at −80 °C. Serum tubes were allowed to warm to room temperature prior to hybridization experiments.

Qualitative simulations of the cross-catalytic system were performed using a DNA-strand-displacement simulator designed for DNA computation [26]. The simulator utilizes a programming language centered on strand-displacement reactions using toeholds and branch migration of DNA structures. The simulator operates with sequence domains, not at the sequence level, and thus does not account for secondary structure within single-stranded DNA segments.

III. Results and Discussion

A. Measurement of DNA Hybridization Kinetics

Hybridization and strand-displacement kinetics using fluorescence resonant energy transfer (FRET) are shown in Fig. 2. For initial tests, the strand F in Fig. 2 is a dye-modified DNA analogue of the miR-451 base sequence that was chosen as it is found at high abundance in normal blood and is nonspecific to cancer [10]. Fig. 2(left) shows the normalized fluorescence intensity of strand F in 1× PBS. Strand Q has a base sequence that is fully complementary to F and in addition has the ten extra base sequence GTAGTGTGGG at the 5′ end that forms an unhybridized toehold when F and Q hybridize to form the complex FQ. As a result, when F and Q hybridize, the 538-nm TET fluorescence emission is quenched by the 531-nm Iowa Black quencher absorption via FRET [27]. This process allows the kinetics of hybridization of F with Q to be followed by monitoring the TET fluorescence intensity, as shown in Fig. 2(middle), where strand Q was added to the solution at ∼7 min. Strand I is fully complementary to Q and, via competitive binding mediated by the toehold, is able to displace F from the FQ complex by a strand-invasion process. The kinetics of this strand-displacement process can be monitored by observing the recovery of fluorescence intensity as the F strands are released from the FQ complex, as shown in Fig. 2(right), where strand I was added at ∼29 min.

TABLE I
Hybridization and Strand-Invasion Rates for the F, Q, and I DNA Strands in Various Solutions

Solution	Hybridization F+Q→FQ	Strand Invasion FQ+I→F+IQ
1×PBS	3.2×10^5	6.5×10^5
10% SDS	6.8×10^5	2.5×10^5
50% serum	5.3×10^5	7.5×10^5
50% serum/10% SDS	--	2.0×10^6

All rates in units of $M^{-1}s^{-1}$. Each strand was present at 50 nM concentration, except for strand invasion in 10% SDS for which each strand was present at a 10-nM concentration.

The rates of hybridization of F with Q and the rates of strand invasion of I into the complex FQ were determined by fitting the data with the appropriate rate equation and are listed in Table I [27]. The hybridization data indicate that hybridization occurs at comparable rates for each of the three cases. The strand-invasion rate constants are within an order of magnitude of each other. In these experiments, each strand was present at 50 nM concentration, except for the case of strand invasion in 10% SDS for which each strand was present at a 10-nM concentration.

It is noted that strand I decays at a rate of 0.024 s^{-1} in pure serum, and it was necessary to take this into account in obtaining the rate constant for strand invasion in the pure serum case. Degradation of the F and Q strands and the FQ complex in serum was considerably slower due to protection provided by the end modifications of these strands and due to the fact that duplex DNA degrades less rapidly in serum than unmodified single-stranded DNA [22]. The entropy-driven catalytic network is based on strand-displacement reactions. These preliminary experiments show that such reactions occur in serum and serum-SDS at rates comparable to those in PBS. These results indicate that catalytic networks tested in PBS buffer should operate successfully in serum-SDS.

B. RNA Hybridization with DNA

An experiment was performed to assess the hybridization of RNA with DNA. Synthetically produced miR-451, RNA having sequence 5′-AAACCGUUACCAUUACUGAGUU-3′, was hybridized with a probe DNA consisting of the complementary sequence with Cy5 dye at the 5′ end and Iowa Black RQ quencher at the 3′ end. This experiment was performed in 1× PBS with the DNA strand at a concentration of 25 nM and the RNA strand at 10 nM. The rate constant, determined by fitting fluorescence intensity versus time curves, was measured to be 3.2×10^5 $M^{-1}s^{-1}$ (data not shown). This rate is comparable to the DNA–DNA hybridization rate between cDNA strands

of length similar to that of the miRNA. Thus, hybridization experiments using the DNA analogs of miRNAs should provide accurate tests of the cross-catalytic system.

C. Toehold-Mediated Strand Invasion by RNA

An experiment was performed to assess the effectiveness of toehold-mediated strand displacement by RNA. In this experiment, the DNA strands 5′-(TET)-AAACCGTTACCATT ACT-3′ (shortened version of F) and 5′-AACTCAGTAATGG TAACGGTTT-(Iowa Black FQ)-3′ (shortened version of Q) were first hybridized together to form a duplex in which the fluorescent dye and the quencher are next to each other at one end of the duplex, and for which, an overhang consisting of the sequence AACTC occurs at the other end. This overhang functions as a toehold to which the synthetically produced miR-451 can attach to initiate strand invasion. The experiment was performed in 1× PBS buffer with the strands at a concentration of 25 nM. From fluorescence intensity versus time data, the rate with which the TET-labeled strand was displaced from the complex was measured to be 7.5×10^3 $M^{-1}s^{-1}$ (data not shown). This rate is roughly one order of magnitude lower than an all DNA-based system having an overhang of five bases [28]. This experiment indicates that DNA hybridization experiments serve as a useful guide for the performance of nucleic-acid-hybridization networks in which some of the strands consist of RNA.

D. DNA and RNA Degradation in Serum and Serum/SDS

As mentioned in Section III-A, unprotected DNA strands are rapidly degraded in serum due to nuclease activity. To assess the effectiveness of SDS in suppressing nuclease activity, an experiment was performed in which the fluorescence intensity of the FQ complex was monitored as a function of time. Should the FQ complex be degraded by nuclease activity, the TET dye or Iowa Black quencher would be released. Hence, monitoring the fluorescence-intensity increase as a function of time provides an indication of the stability of the FQ complex. An experiment was performed in which FQ was added to 1× PBS, 50% serum, 10% SDS, and 50% serum/10% SDS. The fluorescence intensity versus time plots are shown in Fig. 3. Only the 50% serum sample (serum mixed with an equal volume of 1× PBS) showed appreciable fluorescence increase. The fluorescence intensity of the remaining samples was relatively stable with variations attributable to instrument instability. The experiments indicate that SDS is effective in suppressing nuclease activity.

E. Simulation of the Catalytic Network

Prior to experimental testing, operation of the cross-catalytic network was simulated to verify proper design of the DNA strand domains. Simulations were performed using a domain-level strand-displacement computational system designed for DNA [26]. The simulator input file lists the concentration (in arbitrary units) and domain structure of all single-stranded and double-stranded complexes that would be present in solution. Using toehold-mediated strand invasion and branch migration,

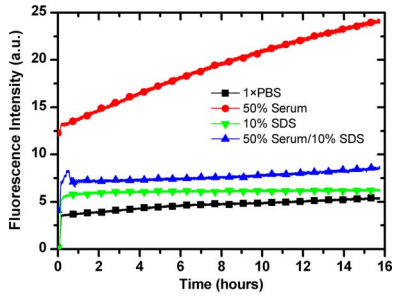

Fig. 3. DNA and RNA degradation in serum and serum-SDS. Degradation of hybridized DNA strands (FQ) was assessed by fluorescence intensity increases as dye-quencher pairs were separated via nuclease activity. Experiments were performed in which FQ was added to 1× PBS, 50% serum, 10% SDS, and 50% serum/10% SDS. The stability of double-stranded DNA was greatly increased in the 50% serum/10% SDS solution.

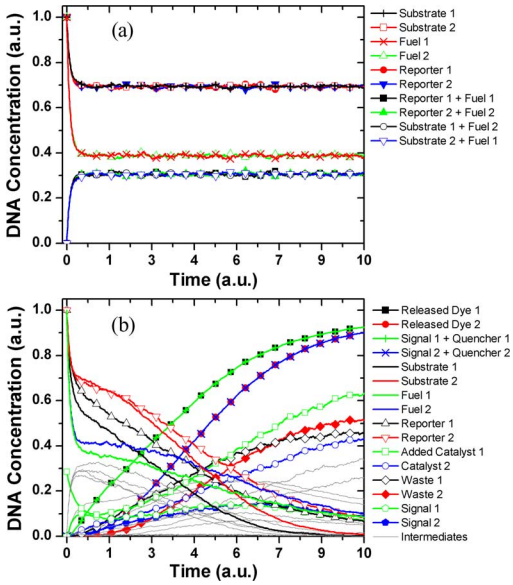

Fig. 4. Simulations of the cross-catalytic network shown in Fig. 1(b)–(d) where "1" refers to components of the left-hand loop and "2" refers to those from the right-hand loop. (a) With no added catalyst (**9 x y 2c**), the DNA complexes are stable in time, forming only complexes that do not release Signal strands. (b) Once the catalyst for substrate 1 is added, the cross-catalytic reactions proceed, rapidly producing large amounts of the dye-labeled strands, along with various other double-stranded complexes.

the simulator then solves for all possible hybridization and invasion reactions. Strand interactions then proceed through the possible reactions for a fixed number of time steps with the resulting concentrations of each single- and double-stranded complex determined by the simulator. Fig. 4(a) shows the simulated cross-catalytic network (with all initial components shown in Fig. 1(b)–(d), i.e., substrates, fuels, and reporters) with no catalyst (**9 x y 2c**) added to the system. In Fig. 4, components labeled with a "1" refer to the left-hand loop of Fig. 1(b) and the reporter of Fig. 1(c), whereas components labeled with a "2" refer to the right-hand loop of Fig. 1(b) and the reporter of Fig. 1(d). Double-stranded substrate/fuel and reporter/fuel complexes are formed; however, no signal strands, and thus, no dye-labeled strands are released, thus indicating that the cross-catalytic network is stable in time.

As seen in Fig. 4(b), once strand **9 x y 2c**, the catalyst for the left-hand half-cycle, is added to the system, the cross-catalytic reactions proceed rapidly, as predicted. Several intermediates and double-stranded complexes are formed; however, the primary result is the rapid release of large amounts of dye-labeled strands from the reporter complexes. The rates and quantities of the released dye-labeled strands are equal to the rates and quantities of signal strands that react with the reporter complexes. The amount of released signal strand is controlled by the quantities of available fuel strands and substrate complexes. Thus, the rate of dye release slows significantly as the fuel and substrates become depleted. Although secondary structure and interference between domains must be accounted for independently from the simulator, these simulation results indicate proper operation of the cross-catalytic system at the domain level.

IV. Conclusion

Levels of specific miRNA in human blood can be used for cancer diagnosis. A cross-catalytic DNA-based chemical amplifier has been designed to amplify specific miRNA in serum. The modular construction of the cross-catalytic system should facilitate design optimization and troubleshooting. Each catalytic loop can be independently operated and tested from the others. All strands not containing the domains **m1** or **m2** can be chosen to have base sequences unrelated to miRNA sequences. As a result, most of the system can be designed and optimized such that only the **m1** and **m2** domains and their complements need to be changed, in order to use the system for the detection of a different miRNA. The modular design will also allow the system to be operated in a variety of modes by leaving out individual components. This cross-catalytic system is attractive for use as a miRNA detector in serum, since the separate system components have long-term stability and cross-catalytic systems exhibiting exponential growth of the catalyst concentration will be driven to completion more rapidly than systems that rely on the turnover of a single catalyst.

In addition to catalytic systems, DNA-based chemical networks that can perform Boolean logic functions have been devised [14], which allow the possibility of building DNA-based miRNA detectors that detect relative concentrations of a particular set of miRNAs. As the presence of specific cancers may be related to relative increased levels of several miRNA, concentration-dependent detection may result in greater selectivity in medical diagnosis through miRNA expression profiling.

DNA kinetics studies were performed in human blood serum with and without SDS. Hybridization rates in all solutions were within one order of magnitude of each other for both DNA and RNA. With 10% SDS, DNA lifetime in serum is increased. Addition of SDS to serum should allow the cross-catalytic system to amplify cancer specific miRNA.

Simulations of the cross-catalytic system indicate that the system remains in a metastable state, until a catalyst DNA strand is added to the system. Once the catalyst strand is added, dye-labeled DNA strands are rapidly released into the solution, providing a large, easily detectable fluorescence signal.

Acknowledgment

The authors would like to thank W. B. Knowlton, E. Winfree, and L. Qian for support and insightful discussions of this paper.

References

[1] World Health Organization. (2009, Feb.). Cancer. [Online]. Available: http://www.who.int/mediacentre/factsheets/fs297/en/print.html
[2] American Cancer Society. (2009). Cancer Facts and Figures 2009. [Online]. Available: http://www.cancer.org/docroot/STT/STT_0.asp
[3] L. He and G. J. Hannon, "MicroRNAs: Small RNAs with a big role in gene regulation," *Nat. Rev. Genet.*, vol. 5, pp. 522–531, Jul. 2004.
[4] R. W. Carthew, "Gene regulation by microRNAs," *Curr. Opin. Genet. Dev.*, vol. 16, pp. 203–208, Apr. 2006.
[5] H.-W. Hwang and J. T. Mendel, "MicroRNAs in cell proliferation, cell death, and tumorigenesis," *Br. J. Cancer*, vol. 94, pp. 776–780, Jun. 2006.
[6] A. Cimmino, G. A. Calin, M. Fabbri, M. V. Iorio, M. Ferracin, M. Shimizu, S. E. Wojcik, R. I. Aqeilan, S. Zupo, M. Dono, L. Rassenti, H. Alder, S. Volinia, C.-g. Liu, T. J. Kipps, M. Negrini, and C. M. Croce, "miR-15 and miR-16 induce apoptosis by targeting BCL2," *Proc. Nat. Acad. Sci. USA*, vol. 102, pp. 13944–13949, Sep. 2005.
[7] L. He, J. M. Thomson, M. T. Hemann, E. Hernando-Monge, D. Mu, S. Goodson, S. Powers, C. Cordon-Cardo, S. W. Lowe, G. J. Hannon, and S. M. Hammond, "A microRNA polycistron as a potential human oncogenes," *Nature*, vol. 435, pp. 828–833, Jun. 2005.
[8] J. A. Chan, A. M. Krichevsky, and K. S. Kosik, "MicroRNA-21 is an antiapoptotic factor in human glioblastoma cells," *Cancer Res.*, vol. 65, pp. 6029–6033, Jul. 2005.
[9] L. Zhang, S. Volinia, T. Bonome, G. A. Calin, J. Greshock, N. Yang, C.-G. Liu, A. Giannakakis, P. Alexiou, K. Hasegawa, C. N. Johnstone, M. S. Megraw, S. Adams, H. Lassus, J. Huang, S. Kaur, S. Liang, P. Sethupathy, A. Leminen, V. A. Simossis, R. Sandaltzopoulos, Y. Naomoto, D. Katsaros, P. A. Gimotty, A. DeMichele, Q. Huang, R. Bützow, A. K. Rustgi, B. L. Weber, M. J. Birrer, A. G. Hatzigeorgiou, C. M. Croce, and G. Coukos, "Genomic and epigenetic alterations deregulate microRNA expression in human epithelial ovarian cancer," *Proc. Nat. Acad. Sci. USA*, vol. 105, pp. 7004–7009, May 2008.
[10] X. Chen, Y. Ba, L. Ma, X. Cai, Y. Yin, K. Wang, J. Guo, Y. Zhang, J. Chen, X. Guo, Q. Li, X. Li, W. Wang, Y. Zhang, J. Wang, X. Jiang, Y. Xiang, C. Xu, P. Zheng, J. Zhang, R. Li, H. Zhang, X. Shang, T. Gong, G. Ning, J. Wang, K. Zen, J. Zhang, and C.-Y. Zhang, "Characterization of microRNAs in serum: A novel class of biomarkers for diagnosis of cancer and other diseases," *Cell Res.*, vol. 18, pp. 997–1006, Oct. 2008.
[11] G. A. Calin and C. M. Croce, "MicroRNA signatures in human cancers," *Nat. Rev. Cancer*, vol. 6, pp. 857–866, Nov. 2006.
[12] J. Lu, G. Getz, E. A. Miska, E. Alvarez-Saavedra, J. Lamb, D. Peck, A. Sweet-Cordero, B. L. Ebert, R. H. Mak, A. A. Ferrando, J. R. Downing, T. Jacks, H. R. Horvitz, and T. R. Golub, "MicroRNA expression profiles classify human cancers," *Nature*, vol. 435, pp. 834–838, Jun. 2005.
[13] S. Volinia, G. A. Calin, C.-G. Liu, S. Ambs, A. Cimmino, F. Petrocca, R. Visone, M. Iorio, C. Roldo, M. Ferracin, R. L. Prueitt, N. Yanaihara, G. Lanza, A. Scarpa, A. Vecchione, M. Negrini, C. C. Harris, and C. M. Croce, "A microRNA expression signature of human solid tumors defines cancer gene targets," *Proc. Nat. Acad. Sci. USA*, vol. 103, pp. 2257–2261, Feb. 2005.
[14] G. Seelig, B. Yurke, and E. Winfree, "Catalyzed relaxation of a metastable DNA fuel," *J. Amer. Chem. Soc.*, vol. 128, pp. 12211–12220, 2006.
[15] D. Y. Zhang, A. J. Turberfield, B. Yurke, and E. Winfree, "Engineering entropy-driven reactions and networks catalyzed by DNA," *Science*, vol. 318, pp. 1121–1125, Nov. 2007.
[16] R. S. Geary, "Antisense oligoncleotide pharmacokinetics and metabolism," *Expert Opin. Drug Metab Toxicol.*, vol. 5, pp. 381–391, Apr. 2009.
[17] M. K. Osako, N. Tomita, H. Nakagami, Y. Kunugiza, M. Yoshino, K. Yuyama, T. Tomita, H. Yoshikawa, T. Ogihara, and R. Morishita, "Increase in nuclease resistance and incorporation of NF-κB decoy oligodeoxynucleotides by modification of the 3′-terminus," *J. Gene Med.*, vol. 9, pp. 812–819, Jul. 2007.
[18] D. A. Di Giusto and G. C. King, "Construction, stability, and activity of multivalent circular anticoagulant aptamers," *J. Biol. Chem.*, vol. 279, pp. 46483–46489, Aug. 2004.

[19] G. Rębowski, M. Wójcik, M. Boczkowska, E. Gendaszewska, M. Soszyoski, G. Bartosz, and W. Niewiarowski, "Antisense hairpin loop oligonucleotides as inhibitors of expression of multidrug resistance-associated protein 1: Their stability in fetal calf serum and human plasma," *Acta Biochim. Polon.*, vol. 48, pp. 1061–1076, 2001.

[20] T. D. Samani, B. Jolles, and A. Laigle, "Best minimally modified antisense oligonucleotides according to cell nuclease activity," *Antisense Nucleic Acid Drug Dev.*, vol. 11, pp. 129–136, Jun. 2001.

[21] R. Piva, E. Lambertini, L. Penolazzi, M. C. Facciolo, A. Lodi, G. Aguiari, C. Nastruzzi, and L. del Senno, "In vitro stability of polymerase chain reaction-generated DNA fragments in serum and cell extracts," *Biochem. Pharmacol.*, vol. 56, pp. 703–708, Sep. 1998.

[22] B. C. F. Chu and E. Orgel, "The stability of different forms of double-stranded decoy DNA in serum and nuclear extracts," *Nucleic Acids Res.*, vol. 20, pp. 5857–5959, Nov. 1992.

[23] R. J. Boado and W. M. Pardridge, "Complete protection of antisense oligonucleotides against serum nuclease degradation by an avidin-biotin system," *Bioconjugate Chem.*, vol. 3, pp. 519–523, Nov. 1992.

[24] J.-P. Shaw, K. Kent, J. Bird, J. Fishback, and B. Froehler, "Modified deoxyoligonucleotides stable to exonuclease degradation in serum," *Nucleic Acids Res.*, vol. 19, pp. 747–750, Feb. 1991.

[25] G. D. Hoke, K. Draper, S. M. Freier, C. Gonzalez, V. B. Driver, M. C. Zounes, and D. J. Ecker, "Effects of phosphorothioate capping on antisense oligonucleotide stability, hybridization and antiviral efficacy versus herpes simplex virus infection," *Nucleic Acids Res.*, vol. 19, pp. 5743–5748, Oct. 1991.

[26] A. Phillips and L. Cardelli, "A programming language for composable DNA circuits," *J. R. Soc. Interface*, vol. 6, pp. S419–S436, Jun. 2009.

[27] L. E. Morrison and L. M. Stols, "Sensitive fluorescence-based thermodynamic and kinetic measurements of DNA hybridization in solution," *Biochemistry*, vol. 32, pp. 3095–3104, Mar. 1993.

[28] B. Yurke and A. P. Mills, Jr., "Using DNA to power nanostructures," *Genet. Program. Evolvable Mach.*, vol. 4, pp. 111–122, Jun. 2003.

Author's photographs and biographies not available at the time of publication.